Title

Systemic GM-CSF Recruits Effector T Cells into the Tumor Microenvironment in Localized Prostate Cancer.

Journal

Cancer immunology research, 4(11)

ISSN

2326-6066

Authors

Wei, Xiao X
Chan, Stephen
Kwek, Serena
et al.

Publication Date

2016-11-01

DOI

10.1158/2326-6066.cir-16-0042

Peer reviewed

HHS Public Access

Author manuscript

Cancer Immunol Res. Author manuscript; available in PMC 2017 November 01.

Published in final edited form as:

Cancer Immunol Res. 2016 November ; 4(11): 948–958. doi:10.1158/2326-6066.CIR-16-0042.

Systemic GM-CSF recruits effector T cells into the tumor microenvironment in localized prostate cancer

Xiao X. Wei[1,2], **Stephen Chan**[1,2], **Serena Kwek**[1,2], **Jera Lewis**[1,2], **Vinh Dao**[1,2], **Li Zhang**[1], **Matthew R. Cooperberg**[1,3], **Charles J. Ryan**[1,2,3], **Amy M. Lin**[1,2,3], **Terence W. Friedlander**[1,2], **Brian Rini**[5], **Christopher Kane**[6], **Jeffry P. Simko**[1,3,4], **Peter R. Carroll**[1,3], **Eric J. Small**[1,2,3], and **Lawrence Fong**[1,2]

[1]University of California, San Francisco Helen Diller Family Comprehensive Cancer Center, San Francisco, CA

[2]Division of Hematology/Oncology

[3]Department of Urology

[4]Department of Anatomic Pathology

[5]Cleveland Clinic Taussig Cancer Institute, Cleveland, OH; Department of Hematology and Medical Oncology

[6]University of California, San Diego, La Jolla, CA; Department of Urology

Abstract

Granulocytic-macrophage colony-stimulating factor (GM-CSF) is used as an adjuvant in cancer vaccine trials and has the potential to enhance antitumor efficacy with immunotherapy; however, its immunologic effects are not fully understood. Here, we report results from a phase 1 study of neoadjuvant GM-CSF in patients with localized prostate cancer undergoing radical prostatectomy. Patients received subcutaneous injections of GM-CSF (250 μg/m^2/day) daily for 2 weeks (Cohort 1; $n = 6$), 3 weeks (Cohort 2; $n = 6$), or 4 weeks (Cohort 3; $n = 6$). Treatment was well tolerated with all grade 1 or 2 adverse events. Two patients had a decline in prostate-specific antigen (PSA) of more than 50%. GM-CSF treatment increased the numbers of circulating mature myeloid dendritic cells, proliferating conventional CD4 T cells, proliferating CD8 T cells, and to a lesser magnitude FoxP3$^+$ regulatory CD4 T cells. Although GM-CSF treatment did not augment antigen-presenting cell localization to the prostate, treatment was associated with recruitment of CD8$^+$ T cells to the tumor. These results suggest that systemic GM-CSF can modulate T-cell infiltration in the tumor microenvironment.

Corresponding author: Lawrence Fong, M.D., University of California, San Francisco, 513 Parnassus Avenue, Room HSE301A, Box 1270, San Francisco, CA 94143-0511. lfong@medicine.ucsf.edu.

NCI trial registration: NCT00305669

Disclosure: The authors do not have any conflicts of interest to declare.

Keywords

Granulocyte-macrophage colony-stimulating factor (GM-CSF); prostate cancer; immunotherapy; neoadjuvant; clinical trial; effector T cells; antigen-presenting cells; tumor microenvironment

Introduction

Prostate cancer remains the most prevalent noncutaneous malignancy and the second leading cause of death in men in the United States (1). Although localized prostate cancer is potentially curable with definitive surgery or radiation, up to one-third of patients treated with curative surgical intent ultimately relapse (2–4). Efforts have been made to study neoadjuvant approaches before radical prostatectomy (RP) to improve clinical outcomes (5). Neoadjuvant immunotherapy strategies are attractive approaches, because immunotherapy is generally well tolerated and may be more effective for patients with less advanced disease and lower disease burden (6). Neoadjuvant studies also provide the opportunity to study treatment effects within the tumor and its microenvironment.

Many immunotherapeutic strategies focus on the generation of T cell–based antitumor immunity, and a subset of these utilize cytokines, whether alone or in combination with other therapeutic agents. Granulocyte-macrophage colony-stimulating factor (GM-CSF, sargramostim, Sanofi) is a pluripotent cytokine that regulates the differentiation and function of granulocytes and macrophages (7), and is an important growth factor and stimulator of dendritic cells (DCs) (8). GM-CSF has been widely utilized as a cancer vaccine adjuvant as well as in combination with immune checkpoint blocking antibodies to facilitate antigen recognition and T-cell expansion (9–12); however, the benefit of GM-CSF remains unclear (13–15).

GM-CSF monotherapy has been studied as an immune modulator in several clinical studies of advanced refractory or biochemically relapsed prostate cancer (16–18). Significant declines in prostate-specific antigen (PSA) were observed in some patients, and sustained responses were seen in a small minority of patients. Although the exact mechanism by which GM-CSF contributes to control of disease remains unclear, clinical benefit of GM-CSF is thought to be mediated by enhanced antitumor immunity. In a follow-up analysis, GM-CSF was associated with a transient increase in the number of circulating monocytes and dendritic cells (18). Although it has not been demonstrated conclusively whether the observed changes are clinically significant, they raise the possibility that the positive clinical responses observed in some advanced prostate cancer patients reflect the ability of GM-CSF to enhance antitumor immunity via a T cell–mediated mechanism.

We have shown that neoadjuvant immunotherapy with sipuleucel-T can enhance the recruitment of T cells to the prostate (19). Utilizing a similar approach for analysis, here we characterize the systemic and tissue-specific immunological effects in a cohort of prostate cancer patients treated with neoadjuvant GM-CSF.

Materials and Methods

Study design

This was a single-center phase 1 study of neoadjuvant GM-CSF prior to planned radical prostatectomy (RP) in patients with localized prostate cancer (NCT00305669). Eligibility criteria included appropriate candidacy for RP, adequate complete blood count, and adequate renal and hepatic functions. Patients were excluded if they had prior prostate cancer–directed therapy (hormonal, radiation, chemotherapy, immunotherapy or other investigational therapy), were on systemic steroids, whose tumors had neuroendocrine or small cell features, or who had evidence of nodal or distant metastasis. During dose escalation, patients received GM-CSF (250 μg/m^2/day subcutaneously) on days 1–14 (Cohort 1), days 1–21 (Cohort 2), or days 1–28 (Cohort 3), with 6 patients in each cohort. A phase 2 dose expansion phase at the maximum tolerated dose (MTD) was originally planned; however, the study was terminated early due to slow accrual. All patients underwent RP within 5 days after the last dose of GM-CSF. Patients who failed to undergo RP within 5 days after the last dose of GM-CSF or withdrew from the study were replaced. All patients who received any dose of GM-CSF were included in the safety analysis. The study protocol was reviewed and approved by the Institutional Review Board at the University of California, San Francisco (UCSF) prior to initiation. Signed informed consents were obtained from all patients at the time of trial enrollment.

Study endpoints

The co-primary endpoints were safety and tolerability of daily GM-CSF prior to RP, and differences in the number of infiltrating $CD11c^+$ and $CD68^+$ antigen-presenting cells (APCs) (number/μm^2) between RP tissues of study patients and RP tissues from untreated control patients, quantified by immunohistochemistry (IHC) and image analysis. Secondary endpoints included differences in the number of infiltrating T-cell subsets ($CD3^+$, cytotoxic $CD3^+CD8^+$, helper $CD4^+$, and regulatory $CD4^+FOXP3^+$ T cells) between RP tissues of treated patients and untreated controls, quantified by IHC and image analysis; treatment-associated changes in circulating immune cell subsets measured by flow cytometry of peripheral blood mononuclear cells (PBMCs); treatment-associated changes in PSA; changes in Gleason scores between pretreatment biopsy and post-treatment RP tissues; and surgical outcomes, including surgical complications and estimated blood loss.

Blood and tissue samples

Whole blood was collected via peripheral venipuncture at baseline (all cohorts), day 14 (all cohorts), and pre-operatively (day 21 for Cohort 2 and day 28 for Cohort 3). PBMCs were isolated from whole blood by ficoll-hypaque density gradient centrifugation. Formalin fixed and paraffin embedded (FFPE) specimens from radical prostatectomy specimens were made available for the current study. Tissues from twelve patients who underwent RP at UCSF without pre-operative therapy, matched to the study patients by the distribution of Cancer of the Prostate Risk Assessment (CAPRA) risk scores, were used as controls.

Flow cytometry

PBMCs were thawed into FACS wash (PBS, 2% BSA) and washed twice with FACS wash. Samples were stained with designated panels for 20 minutes at 4°C and washed twice with FACS wash. Cells requiring intracellular staining were fixed and permeabilized with BD Cytofix/Cytoperm buffer (Cat #554722) according to the manufacturer's protocol. Intracellular staining with antibodies was carried out for 30 minutes at 4°C and washed twice with FACS wash. Cells were acquired on a LSRII flow cytometer (BD Biosciences) and data were analyzed with FlowJo analysis software version 9.7.5 (FlowJo, LLC). DCs were gated from both the lymphocyte and myeloid populations in the forward scatter (FSC)-A by side scatter (SSC)-A plots. Monocytes and granulocytes were gated from the myeloid populations in the FSC-A by SSC-A plots. T cells were gated from the lymphocyte gate in the FSC-A by SSC-A plots. The absolute counts for each cell type were calculated by multiplying (a) the percentage of cells gated with (b) the percentage of the preceding subsets, and (c) absolute monocyte count plus absolute lymphocyte count for DCs; absolute monocyte count for monocytes and MDSCs; and absolute lymphocyte count for T-cell subsets. The absolute monocyte and lymphocyte counts were obtained from the complete blood count with differential of respective patients on the day that blood was drawn. The sources for fluorochrome-conjugated antibodies to human CD3, CD8, CD14, CD11c, CD25, CD45, CD66b, CD69, CD86, CD123, FoxP3, HLA-DR, INOS and Ki-67 are summarized in Supplementary Table 1.

Immunohistochemistry

Immunohistochemistry was performed on 5-μm FFPE sections from RP specimens. For CD68 single staining, slides were incubated with anti-CD68 mouse monoclonal antibody (Dako #M0876, Clone #PG-M1) for 30 to 60 minutes at room temperature, and antigen-antibody complexes were visualized with the EnVision+ Dual Link System-HRP (Dako #K4063). For double stains, slides were first incubated with primary antibody to CD8, FoxP3, or CD83 (Supplementary Table 2) for 30 to 60 minutes at room temperature, and visualized with horseradish peroxidase (HRP) using DAB+ as chromogen (EnVision G|2 Doublestain System; Dako #K5361). This was followed by incubation with secondary antibody to CD3, CD4, or CD11c (Supplementary Table 2) for 60 minutes, and visualized with alkaline phosphatase (AP) using Permanent Red as chromogen (Envision G|2 Doublstain System; Dako #K5361). Specimens were counterstained with hematoxylin prior to analysis. Immune infiltration in RP tissue was evaluated by immunohistochemistry, where tissue was designated into three distinct compartments: benign glands, tumor interface, and tumor center. Five randomly selected fields from each compartment were captured with ImageScope software (Aperio), and automatic cell counts for single- and double-stained cells were determined with AxioVision software (Zeiss, Peabody, MA).

Statistical analysis

Statistical analysis was performed with Prism software Version 6.0. Baseline patient characteristics were compared among cohorts using the Fisher exact test for categorical variables and the Kruskal-Wallis test for continuous variables. Due to the study design, peripheral blood immune subsets data was available at baseline and day 14 for all three

treated cohorts; day 21 for cohort 2 only; and day 28 for cohort 3 only. Pairwise comparisons between each time point were performed by the Wilcoxon matched-pairs signed rank test. To analyze differences in tissue immune cell infiltration by tissue compartment (benign glands, tumor interface, and tumor center), the Wilcoxon matched-pairs signed rank test was also used. The Mann-Whitney test was used to perform comparisons of tissue immune cell infiltration between the untreated controls and each of treated cohorts. Kruskal-Wallis test was implemented to determine whether there was a significant difference among the three treated cohorts, and the Wilcoxon matched-pairs signed rank test was then used to perform pairwise comparisons between treated cohorts if significant. A P value of < 0.05 was considered statistically significant. No multiple testing adjustment was performed.

Results

Patients

Between November 16, 2004 and February 15, 2011, 18 patients were enrolled at UCSF. Overall, 7 (38.9%) patients had low-risk disease, 8 (44.4%) patients had intermediate-risk disease, and 3 (16.7%) patients had high-risk disease (Table 1). Patients were enrolled into Cohort 1 (GM-CSF 250μg/m^2/day s.c. for 14 days), Cohort 2 (GM-CSF 250μg/m^2/day s.c. for 21 days) and Cohort 3 (GM-CSF 250μg/m^2/day s.c. for 28 days), sequentially. Due to the small sample sizes and non-randomized nature of the study, baseline characteristics were not completely balanced among the cohorts. Gleason score and NCCN risk group were statistically different among the cohorts, largely driven by two patients with Gleason 8 disease in Cohort 3 (Table 1). All 18 patients underwent radical prostatectomy (RP) within 5 days of the last GM-CSF injection. Four addition patients who were enrolled were replaced due to delayed RP or withdrawal from the study. One patient had acute Grade 2 hypoxemia during anesthesia for planned RP related to body habitus; surgery was aborted and the patient was taken off of the study. Two patients were removed from the study due to asymptomatic leukocytosis between 30–40 $\times 10^9$/L. One patient withdrew consent in the middle of treatment. All enrolled patients who received any dose of GM-CSF were included in the safety analysis.

Safety

Adverse events (AEs) determined to be related or possibly related to GM-CSF treatment that occurred prior to RP were summarized in all 22 patients. All AEs were Grade 1 or Grade 2 and transient (Table 2). The most common AEs (> 10% of patients) were injection site reaction (81.8%), fatigue (63.6%), bone pain (27.3%), and headache (13.6%). Neoadjuvant GM-CSF treatment did not appear to affect operative complications, duration of surgery, or estimated blood loss during surgery. Leukocytosis was not considered an AE since GM-CSF treatment was anticipated to cause a rise in total white blood cell count.

Clinical correlates

Two patients (11.1%) had a > 50% decline in PSA during neoadjuvant GM-CSF treatment (Fig. 1). One patient in Cohort 1 had baseline PSA of 6.4 ng/mL which decreased to 3.09 ng/mL after 2 weeks of neoadjuvant therapy. A Cohort 3 patient had baseline PSA of 5.1

ng/mL which decreased to 3.8 ng/mL after 2 weeks, then further decreased to 2.4 ng/mL after 4 weeks of therapy,. One patient (5.6%) in Cohort 1 had a > 50% increase in PSA during treatment (Fig. 1), from 4.2 ng/mL to 7.97 ng/mL. Because the baseline PSA values for all patients were relatively low (range: 3.03–13.2 ng/mL), the clinical significance of these PSA changes are unclear. Overall, no significant downstaging was observed at the time of RP. Five patients (27.8%) had downgrading of Gleason scores, and five patients (27.8%) had upgrading of Gleason scores at the time of RP compared to pretreatment biopsies (Supplementary Fig. 1). All patients had pN0 ($n = 11$) or pNX ($n = 7$) disease at the time of RP.

Changes in the peripheral APC compartment

The numbers of circulating dendritic cells and monocytes have been reported to increase after GM-CSF administration in patients (18). There is also preclinical evidence that high doses of GM-CSF may recruit myeloid derived suppressor cells (MDSCs) and impair antitumor immunity (20). In this study, PBMCs from study subjects at baseline (before treatment), day 14, and at completion of treatment (day 21 for Cohort 2, and day 28 for Cohort 3) were stained for APC markers and analyzed by flow cytometry to assess changes in immune subsets during treatment.

The HLA-DR$^+$ dendritic cells (DCs) were separated into myeloid (CD11c$^+$CD123$^-$) and plasmacytoid (CD11c$^-$CD123$^+$) lineages. CD86 positivity was utilized to identify activated and mature dendritic cells. GM-CSF treatment led to a significant decrease in the frequency of circulating myeloid and plasmacytoid DCs at day 14 compared to baseline ($P = 0.0002$ and $P = 0.0151$, respectively) (Fig. 2A and B, **top left panels**). However, the absolute number of myeloid and plasmacytoid DCs (Fig. 2A and B, **top right panels**) and the frequencies and numbers of their respective CD86$^+$ subsets (Fig. 2A and B, **bottom panels**) did not significantly decrease. The absolute number of CD86$^+$ myeloid DCs overall increased from baseline to day 14 ($P = 0.0302$), indicating that the decrease in frequency of dendritic cells did not adversely impact the number of activated dendritic cells.

The frequency of CD14^{hi}HLADR$^+$CD66b$^-$ monocytes overall decreased from baseline to day 14 ($P = 0.0052$); however, the absolute number of these monocytes was not significantly changed (Fig. 2C). The frequency and absolute number of monocytic MDSC (CD14^{hi}HLADR$^-$CD66b$^-$INOS$^+$) did not change significantly with GM-CSF treatment (Fig. 2D).

Changes in the peripheral T-cell compartment

The study hypothesized that GM-CSF induces the uptake and processing of relevant prostate cancer antigens by dendritic cells, which in turn crossprime anti-prostate cancer T cells. The effects of neoadjuvant treatment with GM-CSF on peripheral T-cell subsets were assessed by flow cytometry. PBMCs from trial patients at baseline, day 14, and at completion of treatment were stained for T-cell markers, Ki67 as a proliferative marker, and CD69 as an activation marker.

The administration of GM-CSF did not lead to an overall increase in the frequencies or numbers of total cytotoxic T cells ($CD3^+CD8^+$) (Fig. 3A, **left panel**), or activated cytotoxic T cells ($CD3^+CD8^+CD69^+$) (Fig. 3A, **middle panel**). However, the frequency and number of proliferative cytotoxic T cells ($CD3^+CD8^+Ki67^+$) increased after GM-CSF treatment between baseline and day 14 ($P = 0.0052$ and $P = 0.0125$, respectively) (Fig. 3A, **right panel**). In contrast, the frequencies and numbers of $CD3^+CD8^-$ helper T cells ($P = 0.0002$ and $P = 0.0353$, respectively) (Fig. 3B, **left panel**), activated helper T cells (CD3+CD8−CD69+) ($P < 0.0001$ and $P = 0.0002$, respectively) (Fig. 3B, **middle panel**), and proliferative helper T cells ($CD3^+CD8-Ki67^+$) ($P < 0.0001$ and $P < 0.0001$, respectively) (Fig. 3B, **right panel**) all increased after GM-CSF treatment. Of note, there also appeared to be an increase in the frequency and number of regulatory T cells ($CD3^+CD8^-CD25^+FoxP3^+$) ($P = 0.0182$ and $P = 0.0103$, respectively) (Fig. 3C). Higher ratio of activated $CD3^+CD8^-$ helper T cells to regulatory T cells, as well as proliferative $CD3^+CD8^-$ helper T cells to regulatory T cells were observed from baseline to day 14 ($P = 0.0067$ and $P = 0.0054$, respectively) (Fig. 3D). No significant differences were observed in the ratio of activated and proliferative cytotoxic T cells to regulatory T cells (data not shown). Most of the observed circulating T-cell changes appeared to be transient; differences compared to pre-treatment baseline were most pronounced at day 14.

APC localization in the tumor microenvironment

Untreated control RP and post–GM-CSF RP specimens were stained for the presence of $CD11c^+CD83^+$ dendritic cells and $CD68^+$ macrophages/monocytes. Representative images are shown (Fig. 4A and B, **top panels**). Overall, there was very little APC infiltration within the tumor or its microenvironment, with particularly minimal CD83 staining in both groups. No significant quantitative differences were seen in CD11c and CD68 staining between untreated control RP and post-GM-CSF RP specimens within the tumor interface or tumor (Fig. 4A and B, **bottom panels**). CD11c staining was observed to be lower in the post-GM-CSF RP specimens compared to untreated control RP tissues within the benign peri-tumoral tissue These findings indicate that systemic GM-CSF did not significantly enhance APC localization to the tumor or its microenvironment.

T-cell localization in the tumor microenvironment

RP tissues from untreated controls and study patients treated with GM-CSF were stained for $CD3^+$, $CD3^+CD8^+$, $CD4^+$, and $CD4^+FoxP3^+$ T-cell subsets (Fig. 4C). Immunohistochemical specimens were quantified for positive cells in the benign peri-tumoral tissue, at the tumor interface, and within the tumor center. Overall, the administration of neoadjuvant GM-CSF significantly increased the number of $CD3^+$ cells at the tumor interface, and to a lesser degree in the tumor center (Fig. 4D, **upper left panel**). At the tumor interface, the increase in $CD3^+$ cells were comprised of $CD3^+CD8^+$ cytotoxic T cells (Fig. 4D, **upper right panel**, $p<0.0001$); there was also a trend towards increase in conventional $CD4^+$ T cells (Fig. 4D, **lower left panel**, $P = 0.0646$). In the tumor center, the increase in $CD3^+$ T cells was comprised of both $CD3^+CD8^+$ cytotoxic T cells (Fig. 4D, **upper right panel**, $P = 0.008$) and conventional $CD4^+$ T cells (Fig. 4D, **lower left panel**, $P = 0.008$). Treatment was also associated with an increase in $CD4^+FoxP3^+$ regulatory T cells in the tumor center, although

to a much lower magnitude than cytotoxic or conventional T cells (Fig. 4D, **lower right panel**, $P = 0.0234$).

T-cell localization was analyzed by cohort to assess for any differential effects of GM-CSF by duration of treatment (Fig. 5). An increase in $CD3^+CD8^+$ T-cell infiltration within the tumor interface compared to untreated controls was observed in all cohorts ($P = 0.0268$ for Cohort 1; $P = 0.0008$ for Cohort 2; and $P = 0.0008$ for Cohort 3) (Fig. 5B, **middle panel**). An increase in $CD3^+$, $CD3^+CD8^+$, and $CD4^+$ T-cell infiltration within the tumor center compared to untreated controls was significant only in Cohort 3 ($P = 0.0320$, $P = 0.0182$, and $P = 0.0001$, respectively) (Fig. 5A–C, **right panels**). While small in magnitude, the increase in $CD4^+FoxP3^+$ T-cell infiltration into the tumor interface and center compared to untreated controls was statistically significant only in Cohort 3 ($P = 0.0415$ and $P = 0.0020$, respectively) (Fig. 5D, **middle and right panels**). When comparing the three treated cohorts, differences were observed only in $CD4^+$ T-cell infiltration in the benign peri-tumoral tissue ($P = 0.0010$) and tumor interface ($P = 0.0176$). Specifically, $CD4^+$ T-cell infiltration in the benign peri-tumoral tissue and tumor interface was significantly higher in Cohort 3 compared to shorter-duration treatment cohorts (Fig. 5C, **left and middle panels**). Taken together, these data suggest that whereas peripheral effects of GM-CSF appeared to be transient, longer durations of GM-CSF have differential effects within the tumor microenvironment. It should be noted that in addition to treatment duration, differences in baseline characteristics among study cohorts may have contributed to these observations (Table 1).

Discussion

GM-CSF is a pleotropic cytokine that is FDA-approved for the mobilization of granulocytes (7). The role of GM-CSF has expanded to cancer immunotherapeutics in recent years. Tvec, an attenuated herpes simplex 1 virus (HSV-1) that expresses GM-CSF, is FDA approved for the treatment of metastatic melanoma (21). Sipuleucel-T is an autologous cellular vaccine that is FDA approved for the treatment of asymptomatic or minimally symptomatic metastatic castration-resistant prostate cancer, which consists of autologous PBMCs cultured and activated with a recombinant protein PAP–GM-CSF (22, 23). More recently, GM-CSF combined with local radiotherapy was reported to lead to abscopal responses in 26.8% (95% CI: 14.2, 42.9) patients with metastatic solid tumors (24). Despite these advances, the benefit of GM-CSF remains unclear, in part because of the heterogeneity of different clinical studies, and a lack of direct investigation of the role of GM-CSF.

We have previously shown that GM-CSF monotherapy may possess single-agent activity in advanced prostate cancer (16–18), and is being used as an adjuvant in multiple investigational trials for advanced prostate cancer, including with DNA plasmid vaccines (25, 26) and PROSTVAC, a PSA-targeted poxviral vaccine for prostate cancer (27). The phase 2 randomized controlled trial of PROSTVAC showed promising results, including improvement in overall survival (27). The phase 3 randomized, double-blind study of PROSTVAC with or without GM-CSF is ongoing (NCT01322490), and should provide insights into the contribution of GM-CSF to PROSTVAC vaccination strategy.

In this study, we showed that neoadjuvant GM-CSF administration is well tolerated, and enhances $CD4^+$ and $CD8^+$ T-cell infiltration but not APC recruitment into the tumor microenvironment in prostate cancer patients. In the circulation, systemic GM-CSF administration led to transient increases in mature myeloid dendritic cells, activated $CD8^+$ T cells, and activated and proliferating $CD4^+$ T cells. These results suggest that APCs activate T cells outside of the tumor microenvironment; this may be occurring in the lymphoid tissues, but would need to be formally examined. It is also possible that GM-CSF exerts qualitative effects on APCs by promoting maturation and antigen presentation efficiency, leading to the generation of more effective T-cell responses. To our knowledge, this is the first study to demonstrate that systemic administration of GM-CSF leads to an increase in T-cell infiltration at the tumor site. This study provides a potential immunological mechanism to explain the ability of GM-CSF to control prostate cancer in at least a subset of patients in prior clinical trials (16–18).

Although we have not further characterized the observed T-cell populations in the current study, it is likely that at least some of the infiltrating lymphocytes preferentially home to the tumor site after GM-CSF administration, a portion of which are likely to be of an activated effector T-cell phenotype. Additional studies are needed to further characterize these T-cell populations to conclusively demonstrate if they are tumor-specific, and to determine if they are effective for tumor control. Most likely, clinically significant antitumor immunity will require both sufficient numbers of infiltrating T cells as well as the “right” activation phenotype.

Systemic GM-CSF administration may also impact other immune cell subsets systemically, including dendritic cells (18) and immunosuppressive cells such as regulatory T cells (28) and myeloid-derived suppressor cells (MDSCs) (20). In this paper, we have shown that the number of circulating proliferative $CD8^+$ T cells and regulatory T cells increase following GM-CSF, and the overall frequency of myeloid and plasmacytoid DCs decreased following GM-CSF. Parallel findings were reported in a phase 1 study of Prostate GVAX, consisting of two allogeneic GM-CSF transduced prostate cancer cell lines (LN-CaP and PC3), combined with six infusions of escalating doses of ipilimumab, a monoclonal antibody to CTLA-4, in patients with metastatic castration-resistant prostate cancer (mCRPC) (29, 30). However, given the multiple components in their immunotherapy strategy, it is difficult to attribute the observed changes to GM-CSF alone, and the influence of ipilimumab and the allogeneic cells cannot be discerned. Regardless, these investigators also made the clinically important observation that increases in activated T cells, low frequencies of MDSCs, as well as high DC activation, were predictive for improved overall survival (29, 30). We have not yet correlated changes in immune cell subsets with clinical outcomes in our patient population. Thus, the clinical impact of our observations remains unknown, and will be a focus of future studies.

As in our study with neoadjuvant sipuleucel-T (19), all of the patients on this trial underwent RP shortly after immunological intervention, as specified by the trial protocol. Thus, the kinetics of the T-cell responses after GM-CSF have not been well defined. For example, it is not known how rapidly the activated T cells home to and infiltrate the tumor, and how durable the observed immunological effects may be. In addition, it is not clear if a memory

T-cell response was generated by systemic GM-CSF as given on this trial, given the relatively short follow up of these patients and the absence of long-term immunomonitoring.

Despite the study limitations, our data show the potential for enhancing T cell–mediated immune effects by systemic GM-CSF administration. These results provide the rationale for immunotherapy trials utilizing GM-CSF in combination with other immunologic agents. In particular, systemic GM-CSF may help to convert a “non-inflamed” tumor microenvironment to an “inflamed” tumor microenvironment comprised of infiltrating T cell, leading to more effective tumor control. Future studies should further investigate the role of GM-CSF, including varying effects of different dosing schedules. Clinical development of combination strategies involving GM-CSF should include a control arm lacking GM-CSF, when possible. Careful design of immunomonitoring protocols, both in the peripheral and tumor compartments, may help to identify features of the immune response that serve as useful biomarkers to predict tumor control and long-term clinical outcomes.

Supplementary Material

Refer to Web version on PubMed Central for supplementary material.

Acknowledgments

SC, JL, and LF were supported by NIH 1R01 CA136753. SK was supported by the Peter Michael Foundation. LF and LZ were supported by NIH 1R01 CA163012. We thank all patients and their families who participated in this study.

References

1. Siegel RL, Miller KD, Jemal A. Cancer Statistics, 2015. CA Cancer J Clin. 2015; 65:5–29. [PubMed: 25559415]
2. Ohori M, Goad JR, Wheeler TM, Eastham JA, Thompson TC, Scardino PT. Can radical prostatectomy alter the progression of poorly differentiated prostate cancer? J Urol. 1994; 152:1843–1849. [PubMed: 7523732]
3. Catalona WJ, Smith DS. 5-year tumor recurrence rates after anatomical radical retropubic prostatectomy for prostate cancer. J Uro. 1994; 152:1837–1842.
4. Zincke H, Oesterling JE, Blute ML, Bergstralh EJ, Myers RP, Barrett DM. Long-term (15 years) results after radical prostatectomy for clinically localized (stage T2c or lower) prostate cancer. J Urol. 1994; 152:1850–1857. [PubMed: 7523733]
5. Pietzk EJ, Eastham JA. Neoadjuvant treatment of high-risk, clinically localized prostate cancer prior to radical prostatectomy. Curr Urol Rep. 2016; 17:37. [PubMed: 26968417]
6. Schellhammer PF, Chodak G, Whitmore JB, Sims R, Frohlich MW, Kantoff PW. Lower baseline prostate-specific antigen is associated with a greater overall survival benefit from sipuleucel-T in the Immunotherapy for Prostate Adenocarcinoma Treatment (IMPACT) trial. Urology. 2013; 81:1297–1302. [PubMed: 23582482]
7. Markowicz S, Engleman EG. Granulocyte-macrophage colony-stimulating factor promotes differentiation and survival of human peripheral blood dendritic cells in vitro. J Clin Invest. 1990; 85:955–961. [PubMed: 2179270]
8. Waller EK. The role of sargramostim (rhGM-CSF) as immunotherapy. Oncologist. 2007; 12(Suppl 2):22–26.
9. Van den Eertwegh AJ, Versluis J, van den Berg HP, Santegoets SJ, van Moorselaar RJ, van der Sluis TM, et al. Combined immunotherapy with granulocyte-macrophage colony-stimulating factor-

transduced allogeneic prostate cancer cells and ipilimumab in patients with metastatic castration-resistant prostate cancer: a phase 1 dose-escalation trial. Lancet Oncol. 2012; 13:509–517. [PubMed: 22326922]

10. Hodi FS, Lee S, McDermott DF, Rao UN, Butterfield LH, Tarhini AA, et al. Ipilimumab plus sargramostim vs ipilimumab alone for treatment of metastatic melanoma: a randomized clinical trial. JAMA. 2014; 312:1744–1753. [PubMed: 25369488]
11. Hodi FS, Butler M, Oble DA, Seiden MV, Haluska FG, Kruse A, et al. Immunologic and clinical effects of antibody blockade of cytotoxic T lymphocyte-associated antigen 4 in previously vaccinated cancer patients. Proc Natl Acad Sci U. S. A. 2008; 105:3005–3010. [PubMed: 18287062]
12. Kwek SS, Lewis J, Zhang L, Weinberg V, Greaney SK, Harzstark AL, et al. Preexisting levels of CD4 T cells expressing PD-1 are related to overall survival in prostate cancer patients treated with ipilimumab. Cancer Immunol Res. 2015; 3:1008–1016. [PubMed: 25968455]
13. Parmiani G, Castelli C, Pilla C, Santinami M, Colombo MP, Rivoltini L. Opposite immune functions of GM-CSF administered as vaccine adjuvant in cancer patients. Ann Oncol. 2007; 58:226–232.
14. Faires MB, Hsueh EC, Ye X, Hoban M, Morton DL. Effect of granulocyte/macrophage colony-stimulating factor on vaccination with an allogeneic whole-cell melanoma vaccine. Clin Cancer Res. 2009; 15:7029–7035. [PubMed: 19903777]
15. Slingluff CL, Petroni GR, Olson WC, Smolkin ME, Ross MI, Haas NB, et al. Effect of granulocyte/macrophage colony-stimulating factor on circulating CD8+ and CD4+ T-cell responses to a multipeptide melanoma vaccine: outcomes of a multicenter randomized trial. Clin Cancer Res. 2009; 15:7036–7044. [PubMed: 19903780]
16. Small EJ, Reese DM, Um B, Whisenant S, Dixon SC, Figg WD. Therapy of advanced prostate cancer with granulocyte macrophage colony-stimulating factor. Clin Cancer Res. 1999; 5:1738–1744. [PubMed: 10430077]
17. Rini BI, Weinberg V, Bok R, Small EJ. Prostate-specific antigen kinetics as a measure of the biologic effect of granulocyte-macrophage colony-stimulating factor in patients with serologic progression of prostate cancer. J Clin Oncol. 2003; 21:99–105. [PubMed: 12506177]
18. Rini BI, Fong L, Weinberg V, Kavanaugh B, Small EJ. Clinical and immunological characteristics of patients with serologic progression of prostate cancer achieving long-term disease control with granulocyte-macrophage colony-stimulating factor. J Urol. 2006; 175:2087–2091. [PubMed: 16697809]
19. Fong L, Carroll P, Weinberg V, Chan S, Lewis J, Corman J, et al. Activated lymphocyte recruitment into the tumor microenvironment following preoperative sipuleucel-T for localized prostate cancer. J Natl Cancer Inst. 2014; 106 dju268.
20. Serafini P, Carbley R, Noonan K, Tan G, Bronte V, Borrello I. High-dose granulocyte-macrophage colony-stimulating factor-producing vaccines impair the immune response through the recruitment of myeloid suppressor cells. Cancer Res. 2004; 64:6337–6343. [PubMed: 15342423]
21. Andtbacka RH, Kaufman HL, Collichio F, Amatruda T, Senzer N, Chesney J, et al. Talimogene Laherparepvec Improves Durable Response Rate in Patients With Advanced Melanoma. J Clin Oncol. 2015; 33:2780–2788. [PubMed: 26014293]
22. Kantoff PW, Higano CS, Shore ND, Berger ER, Small EJ, et al. Sipuleucel-T immunotherapy for castration-resistant prostate cancer. N Engl J Med. 2010; 363:411–422. [PubMed: 20818862]
23. Wei XX, Fong L, Small EJ. Prostate Cancer Immunotherapy with Sipuleucel-T: Current Standards and Future Directions. Expert Rev Vaccines. 2015; 14:1529–1541. [PubMed: 26488270]
24. Golden EB, Chhabra A, Chachoua, Adams S, Donach M, et al. Local radiotherapy and granulocyte-macrophage colony-stimulating factor to generate abscopal responses in patients with metastatic solid tumours: a proof-of-principle trial. Lancet Oncol. 2015; 16:795–803. [PubMed: 26095785]
25. Pavlenko M, Roos A-K, Lundqvist A, Palmborg A, Miller AM, Ozenci V, et al. A phase I trial of DNA vaccination with a plasmid expressing prostate-specific antigen in patients with hormone-refractory prostate cancer. Br J Cancer. 2004; 91:688–694. [PubMed: 15280930]

26. Miller AM, Ozenci A, Kiessling R, Pisa P. Immune monitoring in a phase 1 trial of a PSA DNA vaccine in patients with hormone-refractory prostate cancer. J Immunother. 2005; 28:389–395. [PubMed: 16000958]

27. Kantoff PW, Schuetz T, Blumenstein BA, Glode LM, Bilhartz DL, Wyand M, et al. Overall survival analysis of a phase II randomized controlled trial of a Poxviral-based PSA-targeted immunotherapy in metastatic castration-resistant prostate cancer. J Clin Oncol. 2010; 28:1099–1105. [PubMed: 20100959]

28. Vasu C, Dogan RN, Holterman MJ, Prabhakar BS. Selective induction of dendritic cells using granulocyte macrophage-colony stimulating factor, but not fms-like tyrosine kinase receptor 3-ligand, activates thyroglobulin-specific CD4+/CD25+ T cells and suppresses experimental autoimmune thyroiditis. J Immunol. 2003; 170:5511–5522. [PubMed: 12759428]

29. Santegoets SJ, Stam AG, Lougheed SM, Gall H, Scholten PE, Reijm M, et al. T cell profiling reveals high $CD4^{+}CTLA\text{-}4^{+}$ T cell frequency as dominant predictor for survival after prostate GVAX/ipilimumab treatment. Cancer Immunol Immunother. 2013; 62:245–256. [PubMed: 22878899]

30. Santegoets SJ, Stam AG, Lougheed SM, Gall H, Jooss K, Sacks N, et al. Myeloid derived suppressor and dendritic cell subsets are related to clinical outcome in prostate cancer patients treated with GVAX and ipilimumab. J Immunother Cancer. 2014; 2:31. [PubMed: 26196012]

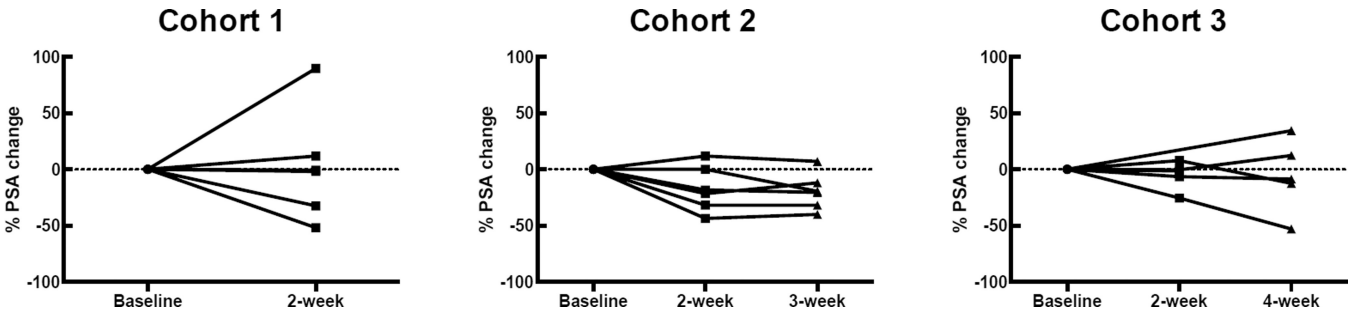

Figure 1. Percent PSA change from baseline by cohort

Cohort 1: GM-CSF, 250 μg/m^2/day s.c. for 14 days. Cohort 2: GM-CSF, 250 μg/m^2/day s.c. for 21 days. Cohort 3: GM-CSF, 250 μg/m^2/day s.c. for 28 days. PSA, prostate specific antigen.

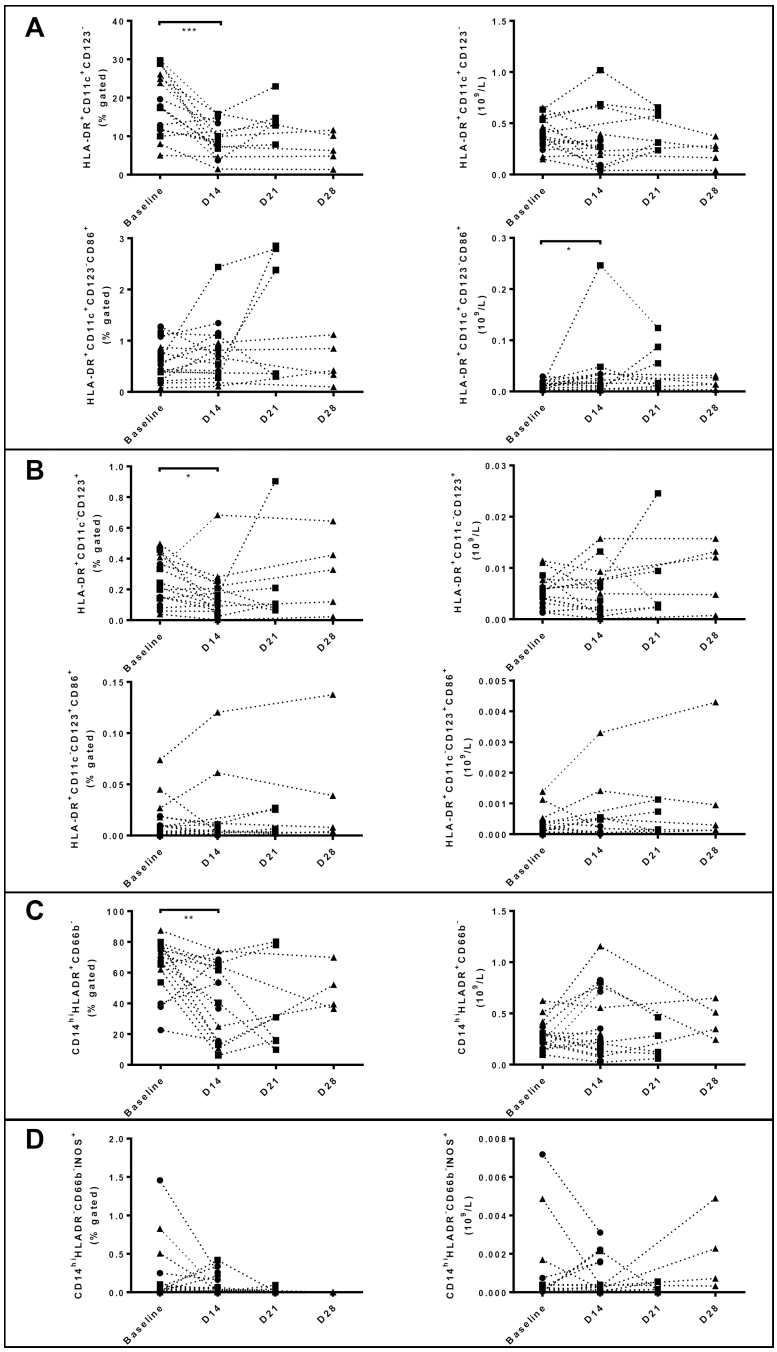

Figure 2. Changes in peripheral DC, monocyte, and MDSC subsets

$HLADR^+CD11c^+CD123^-$ myeloid DCs (Panel A), $HLADR^+CD11c^-CD123^+$ plasmacytoid DCs (Panel B), and their respective mature subsets (lower panels) are expressed in terms of frequency among gated PBMCs (left panels), and as absolute numbers (right panels). $CD14^{hi}HLADR^+CD66b^-$ monocytes (Panel C) and $CD14^{hi}HLADR^-CD66b^-INOS^+$ monocytic MDSC (Panel D) are shown as frequencies among gated PBMCs (left panels), and as absolute counts (right panels). Circle: Cohort 1, Square: Cohort 2, Triangle: Cohort 3. * $P < 0.05$, ** $P < 0.01$, *** $P < 0.001$.

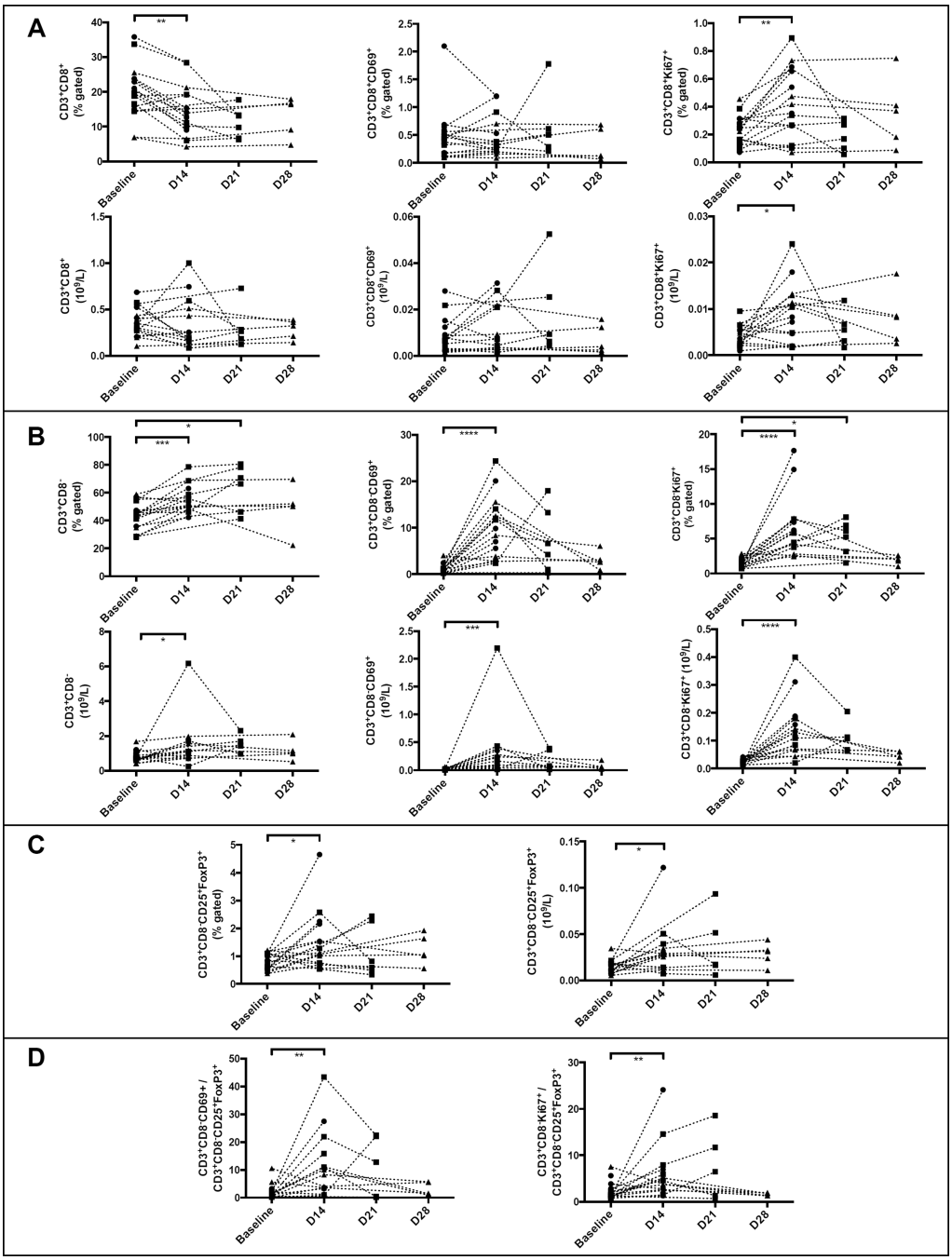

Figure 3. Changes in peripheral T-cell subsets

$CD3^+CD8^+$ cytotoxic T cells (Panel A), $CD3^+CD8^-$ helper T cells (Panel B), and $CD3^+CD8^-CD25^+FoxP3^+$ regulatory T cells (Panel C) are expressed in terms of frequency among gated PBMCs, and as absolute numbers. The ratio of activated and proliferative $CD3^+CD8^-$ helper T cells to regulatory T cells are shown in Panel D. Circle: Cohort 1, Square: Cohort 2, Triangle: Cohort 3. * $P < 0.05$, ** $P < 0.01$, *** $P < 0.001$, **** $P < 0.0001$.

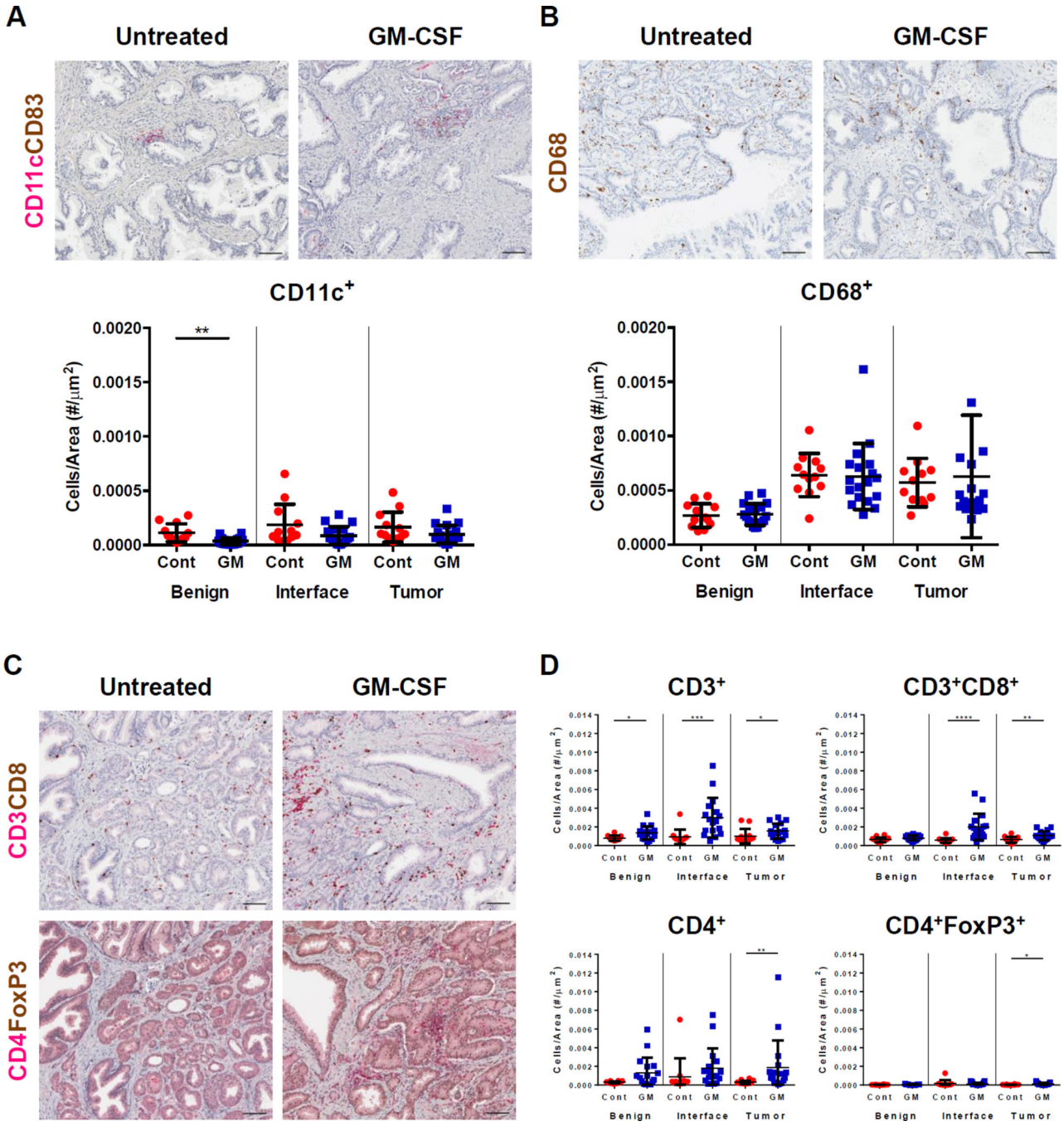

Figure 4. APC infiltration and T-cell infiltration in tissue compartments

CD11c and CD83 immunohistochemical double staining is shown in RP tumor specimens obtained from untreated and GM-CSF–treated patients (Panel A upper), with quantitation of $CD11c^+$ events (Panel A lower). CD68 immunohistochemical single staining is shown in tumor specimens from untreated and GM-CSF–treated patients (Panel B upper), with quantitation of $CD68^+$ events (Panel B lower). Immunohistochemical double stains of CD3 and CD8 (Panel C upper) and CD4 and FoxP3 (Panel C lower) in RP tumor specimens obtained from untreated and GM-CSF–treated patients. Quantitation of $CD3^+$ (Panel D

upper left), $CD3^+CD8^+$ (Panel D upper right), $CD4^+$ (Panel D lower left), and $CD4^+FoxP3^+$ (Panel D lower right) subsets is shown. Scale bar, 100 μm. * $P < 0.05$, ** $P < 0.01$, *** $P < 0.001$, **** $P < 0.0001$.

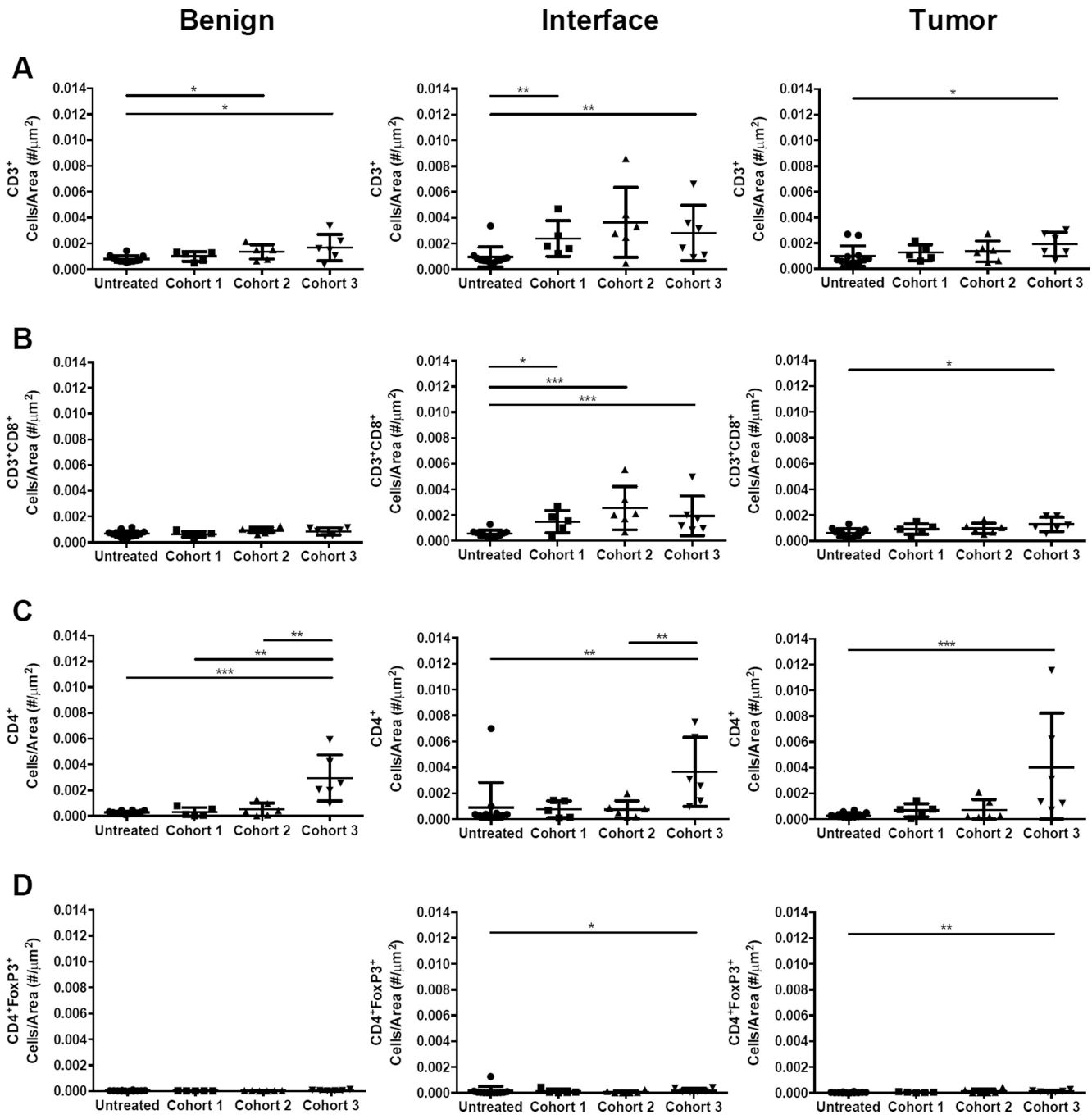

Figure 5. Comparison of T-cell infiltration in tissue compartments across treatment cohorts

Frequencies of $CD3^+$ (Panel A), $CD3^+CD8^+$ (Panel B), $CD4^+$ (Panel C) and $CD4^+FoxP3^+$ (Panel D) T-cell subsets are quantitated in benign peri-tumoral tissues (left panels), at the tumor interface (middle panels), and within the tumor center (right panels) in untreated patients and patients treated with GM-CSF by study cohort. * $P < 0.05$, ** $P < 0.01$, *** $P < 0.001$.

Table 1

Baseline demographics and disease characteristics.

	Cohort 1 (N=6)	Cohort 2 (N=6)	Cohort 3 (N=6)	Total	p-value
Age, year					0.150
Median	60	57	63	60	
Range	57–66	51–63	53–68	51–68	
Weight, lbs					0.103
Median	196.2	228.4	188.4	202.3	
Range	159.7–224.3	178.5–269.9	151.2–227.3	151.2–269.9	
Race, No. (%)					1.000
Caucasian	6 (100.0)	6 (100.0)	6 (100.0)	18 (100.0)	
ECOG					1.000
PS = 0	6 (100.0)	6 (100.0)	6 (100.0)	18 (100.0)	
Gleason sum, No. (%)					0.023
≤6	2 (33.3)	1 (16.7)	4 (66.7)	7 (38.9)	
7	4 (66.7)	5 (83.3)	0 (0.0)	9 (50.0)	
≥8	0 (0.0)	0 (0.0)	2 (33.3)	2 (11.1)	
Clinical stage, No. (%)					0.100
T1c	2 (33.3)	5 (83.3)	2 (33.3)	9 (50.0)	
T2a	4 (66.7)	0 (0.0)	3 (50.0)	7 (38.9)	
T3a	0 (0.0)	1 (16.7)	1 (16.7)	2 (11.1)	
PSA, ng/mL					0.466
Median	5.7	5.9	4.2	5.0	
Range	3.0–9.1	3.6–13.2	3.2–8.9	3.0–13.2	
LDH, U/L					0.927
Median	151	139	151	150	
Range	128–170	129–237	95–199	95–237	
Hemoglobin, g/dL					0.654
Median	15.1	15.4	15.1	15.2	
Range	14.3–15.5	14.7–16.9	12.6–15.9	12.6–16.9	
Alkaline phosphatase, U/L					0.548

	Cohort 1 (N=6)	Cohort 2 (N=6)	Cohort 3 (N=6)	Total	p-value
Median	68	65	75	72	
Range	46–112	47–88	50–97	46–112	
NCCN risk group, No. (%)					0.007
Low	2 (33.3)	1 (16.7)	4 (66.7)	7 (38.9)	
Intermediate	4 (66.7)	4 (66.7)	0 (0.0)	8 (44.4)	
High	0 (0.0)	1 (16.7)	2 (33.3)	3 (16.7)	

Abbreviations: ECOG = Eastern Cooperative Oncology Group; LDH lactate dehydrogenase; PSA = prostate specific antigen.

Table 2

Summary of on-study adverse events

Patients could have had more than one adverse event. No grade ≥3 adverse events were observed.

Adverse events, No. (%)	Grade 1	Grade 2	Total
Injection site reaction	17 (77.3)	1 (4.5)	18 (81.8)
Fatigue	13 (59.1)	1 (4.5)	14 (63.6)
Bone pain	5 (22.7)	1 (4.5)	6 (27.3)
Headache	3 (13.6)	0 (0.0)	3 (13.6)
Back pain	2 (9.1)	0 (0.0)	2 (9.1)
Extremity pain	2 (9.1)	0 (0.0)	2 (9.1)
Muscle pain	1 (4.5)	1 (4.5)	2 (9.1)
Diarrhea	1 (4.5)	0 (0.0)	1 (4.5)
Abdominal pain	1 (4.5)	0 (0.0)	1 (4.5)
Fever (non-neutropenic)	1 (4.5)	0 (0.0)	1 (4.5)
Chills	1 (4.5)	0 (0.0)	1 (4.5)
Diaphoresis	1 (4.5)	0 (0.0)	1 (4.5)
Rash	1 (4.5)	0 (0.0)	1 (4.5)
Chest pain	1 (4.5)	0 (0.0)	1 (4.5)
Joint pain	1 (4.5)	0 (0.0)	1 (4.5)
Pruritus	1 (4.5)	0 (0.0)	1 (4.5)
Urinary frequency	1 (4.5)	0 (0.0)	1 (4.5)
Urinary incontinence	1 (4.5)	0 (0.0)	1 (4.5)
Dehydration	1 (4.5)	0 (0.0)	1 (4.5)
Hoarseness	1 (4.5)	0 (0.0)	1 (4.5)